Mineralogical Magazine, December 2008, Vol. 72(6), pp. 1163–1179

Crystal chemistry and location of hydrogen atoms in prehnite

T. A. Detrie[1], N. L. Ross[1], R. J. Angel[1] and M. D. Welch[2]

[1] Crystallography Laboratory, Department of Geosciences, Virginia Polytechnic Institute and State University, Blacksburg, VA 24061, USA
[2] Department of Mineralogy, The Natural History Museum, Cromwell Road, London SW7 5BD, UK

[*Received 20 November 2008; Accepted 17 February 2009*]

ABSTRACT

The structure of prehnite $Ca_2Al(AlSi_3O_{10})(OH)_2$, including H positions, has been determined by a combination of single-crystal X-ray diffraction and neutron powder diffraction on four natural samples. The symmetry of the average structure with Al/Si disordered at the *T*2 site is *Pncm*. However, for four of the crystals studied, numerous violations of the *n*- and *c*-glide reflection conditions indicate lower symmetry corresponding to space groups *P*2*cm* and *P*2/*n* and Al-Si ordered structures, possibly as domains of different symmetries and ordering within a single crystal. Time-of-flight neutron powder diffraction was carried out on a sample from Mali at 293 K and 2 K. The structure was refined in space group *Pncm* by Rietveld analysis. Although it was not possible to locate the missing H using the 293 K neutron data, these data were used to refine the H position located approximately by single-crystal XRD and to refine U_{iso}. For the 2 K neutron powder diffraction data, H was located directly by difference-Fourier synthesis and its refined position found to be in close agreement with that obtained by the combined XRD/neutron 293 K dataset.

Keywords: prehnite, crystal chemistry, hydrogen, neutron diffraction, XRD, Rietveld.

Introduction

Prehnite, with an ideal formula $Ca_2(Al,Fe,Mn)(AlSi_3O_{10})(OH)_2$, contains corner-sharing tetrahedra and octahedra, with hydroxyl groups located on opposite apices of the $Al[O_4(OH)_2]$ octahedron. The tetrahedra and octahedra form layers, as viewed down the *b* axis, consisting of one octahedral layer and three tetrahedral layers, repeating every 9.3 Å (Fig. 1). The prehnite structure has similarities with framework silicates in that four tetrahedra (two unique sites) are oriented in a corner-sharing corkscrew pattern, extended along [010]. The two unique tetrahedral sites, *T*1 and *T*2, contain Si and Al/Si respectively (Fig. 1). The octahedron, *M*1, contains Al. Any Fe^{3+} in the structure also occupies this site (Artioli *et al.*, 1995; Akasaka *et al.*, 2003). There is a channel in the structure, parallel to [100], where a Ca atom resides in 7-fold coordination (Fig. 2).

The average structure of prehnite has *Pncm* symmetry (Peng *et al.*, 1959), with the *T*1 tetrahedral site fully occupied by Si, whereas *T*2 contains disordered 0.5 Al and 0.5 Si. Papike and Zoltai (1967) showed that there are three possible ordering schemes of the Al and Si on the *T*2 site (Fig. 1). The first has *P*2*cm* symmetry and a distinct Al-rich *T*2 site on the same side of the two tetrahedral corkscrews within the unit cell (Fig.1). In the *P*2/*n* scheme, the Al-rich *T*2 tetrahedron is on opposite sides of the two tetrahedral corkscrews. The last possible scheme, $P22_12$, can be described as having two Al-rich *T*2 tetrahedra in the top corkscrew, and two Si-rich *T*2 tetrahedra in the bottom corkscrew. As pointed out by Papike and Zoltai (1967), the $P22_12$ configuration is unlikely to occur because it results in Al−O−Al linkages (Lowenstein, 1954). Successful refinements in *P*2*cm* symmetry were reported by Balić-

* E-mail: taddet@vt.edu
DOI: 10.1180/minmag.2008.072.6.1163

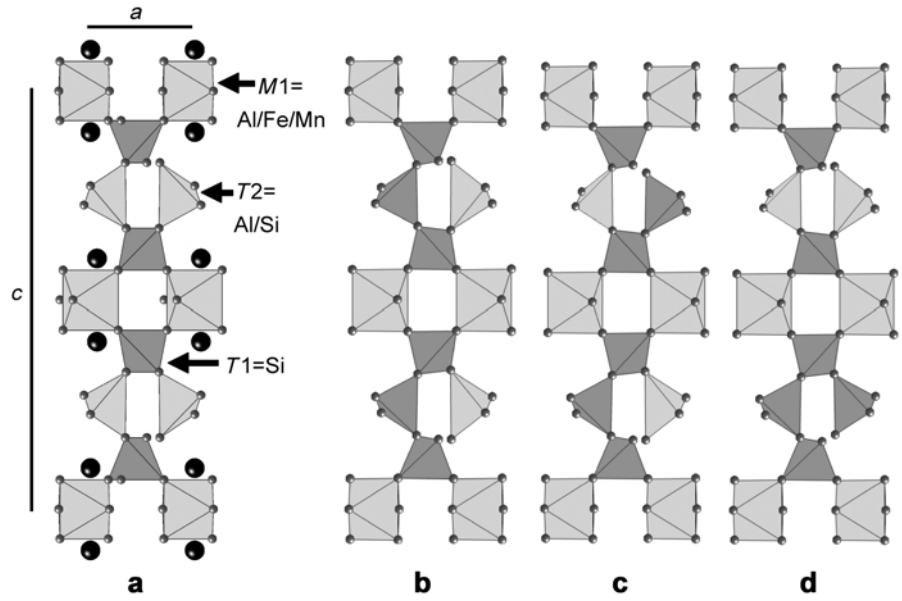

FIG. 1. The ordering schemes of the prehnite structure, as viewed 6º from [010]. The light grey polyhedra represent Al, whereas the dark grey polyhedra represent Si (unless noted otherwise). (*a*) *Pncm* symmetry. The large black spheres represent Ca sites, whereas the small grey spheres represent O sites. (*b*) *P*2*cm* symmetry (c) *P*2/*n* symmetry, *a*-unique (*d*) $P22_12$ symmetry. Modified after Papike and Zoltai (1967).

Žunić *et al.* (1990), Baur and Hofmeister (1990), Aumento (1968), Preisinger (1965), and Nuffield (1943). Space group *P*2*cm* (acentric) is in agreement with the pyroelectric studies performed by Traube (1894), which showed that the [100] direction of prehnite is a polar direction. The presence of twin lamellae or domains with symmetry *P*2/*n* produced during growth was considered a possibility by Akizuki (1987) and Akasaka *et al.* (2003).

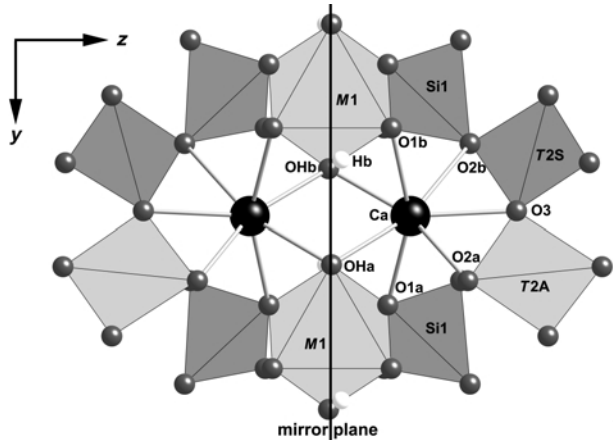

FIG. 2. The Ca channel in prehnite as viewed from a direction 2º from [100] with *P*2*cm* atom labelling. The large black spheres represent Ca sites, the small grey spheres represent O sites, and the small white spheres represent H sites with OH−H vectors perpendicular to the viewing plane. In looking at the labelling and comparing it to *Pncm* atom labelling, the O1a and O1b become one site, the O2a and O2b become one site (O2), the OHa and OHb become one site (OH), and *T*2A and *T*2S become one site (Al/Si disordered *T*2 site).

The location of H in prehnite has not been reported previously, although it can be inferred that it is attached to an otherwise under-bonded oxygen atom that forms the apex of the octahedron, and which is not bonded to either of the tetrahedral sites. This site has consistently been labelled 'OH' in previous structural studies (e.g. Papike and Zoltai, 1967; Balić-Žunić *et al.*, 1990). A definitive location of the H atoms will contribute to the understanding of the thermodynamic properties of prehnite, including the potential for H disorder and the existence, orientation and strength of H-bonding. Neutron powder diffraction studies have succeeded in locating H atoms in mineral structures, including leucophoenicite (Welch *et al.*, 2002), chondrodite (Berry and James, 2002) and akaganéite (Post *et al.*, 2003). These studies used undeuterated samples to eliminate the possibility of incomplete H/D exchange and consequently near-contrast-matched ratios, which would make the H invisible to neutron diffraction. As pointed out by Salvadó *et al.* (1996), the significant background arising from incoherent scattering from H is not necessarily a problem for Rietveld refinement because all background contributions are included, either by interpolation or appropriate refinement of the background. As will be seen in this study, the H content of prehnite presented no difficulties in modelling the background.

The purpose of this study was thus twofold:

(1) to determine whether or not there are significant differences in the state of Al-Si order in prehnite from different localities, and

(2) to locate the H atom in the structure.

Experimental

Prehnite samples from four different localities were used in this study (Table 1). The composition of sample tad5 was provided by G.D. Gatta. Electron microprobe analyses of the other samples were performed on grain mounts with a Cameca SX50 instrument, using CaO, SiO_2, Al_2O_3, Fe_2O_3 and Mn_2O_3 as standards. Chemical compositions were calculated assuming that all Fe and Mn were in the +3 valence state, and H_2O was calculated by difference.

Single-crystal X-ray diffraction (XRD)

Single crystals of each of the four samples were selected for intensity-data collection on the basis of diffraction quality. Rejected crystals typically exhibited split rows of diffraction spots due to misalignment of {001} plates as described by Balić-Žunić *et al.* (1990). Intensity datasets were collected from selected crystals at room conditions with Oxford Diffraction Xcalibur or Gemini diffractometers equipped with CCD detectors, operated at 50 kV and 40 mA, with Mo-$K\alpha$ radiation and a graphite monochromator. Full spheres of diffraction data were collected to 60º2θ. Data were absorption-corrected within the *CrysAlis* program (Oxford Diffraction, 2006). Structure refinements (neutral atom scattering factors) were carried out using *SHELXL-97* (Sheldrick, 2008) driven by *WinGX* (Farrugia, 1999), and using a starting model based on the structure refined in space group *Pncm* by Papike and Zoltai (1967). All sites were assumed to be fully occupied. The Al/Si occupancies of the tetrahedral sites were assigned on the basis of bond lengths. The Fe or Mn were assigned (Artioli *et al.*, 1995; Akasaka *et al.*, 2003) to the octahedral sites, *M*1, and the Al/(Fe+Mn) ratio on these sites was refined. All non-H atoms were refined anisotropically. The hydrogen atoms were located in the difference-Fourier map and subsequently refined, with the O−H distance constrained to 0.98±0.03 Å. Further details of the data collection and subsequent refinements are given in Table 1. The coordinates of the atoms, bond lengths, and bond angles are listed in Tables 2, 3 and 4, respectively, for *Pncm*. The refinement results in *P*2*cm* symmetry are given in Table 5, and atom coordinates, bond lengths, and bond angles can be found in Tables 6, 7 and 8.

Neutron powder diffraction

Experiments were carried out at 293 K and 1.7 K (in a cryofurnace) using the same powder sample of tad4 from the Mali locality. In both cases datasets were collected from the 90º (resolution $\Delta d/d$ = 0.007) and 145º ($\Delta d/d$ = 0.005) detector banks, and data from these banks were refined together using GSAS (Larson and Von Dreele, 2000). Refinement details are summarized in Table 1.

293 K dataset

Neutron diffraction data were collected at room temperature from a powdered sample of prehnite tad4, loaded in a vanadium can and mounted on the POLARIS neutron time-of-flight diffractometer at ISIS, Rutherford-Appleton Laboratory, UK. The diffraction pattern was measured using

TABLE 1. Details of prehnite structure refinements in *Pncm*.

Sample ID Museum, number	tad1x2, Tyrol NHM, BM 1916.641	tad2x1, Norway NHM, OH-BM 3455	tad5x1, South Africa Pagano coll. #8789	tad4x1, Mali purchased	tad4 N- 293 K, Mali purchased	tad4 N- 2 K, Mali purchased
Microprobe	$Ca_{2.06}(Al_{0.93},Fe_{0.07})$	$Ca_{2.05}(Al_{0.997},Mn_{0.003})$	$Ca_{2.07}(Al_{0.98},Mn_{0.02})$	$Ca_{1.92}(Al_{0.74},Fe_{0.26})$	$Ca_{1.92}(Al_{0.74},Fe_{0.26})$	$Ca_{1.92}(Al_{0.74},Fe_{0.26})$
results (±0.01)	$(AlSi_{3.09})O_{11}$	$(AlSi_{3.09})O_{11}$	$(AlSi_{3.09})O_{11}$	$(AlSi_{2.95})O_{11}$	$(AlSi_{2.95})O_{11}$	$(AlSi_{2.95})O_{11}$
Temperature	293(2) K	293(2) K	293(2) K	293(2) K	293(2) K	2 K
Source/Wavelength/ToF	Mo-$K\alpha$ (0.71073 Å)	Mo-$K\alpha$ (0.71073 Å)	Mo-$K\alpha$ (0.71073 Å)	Mo-$K\alpha$ (0.71073 Å)	neutrons ToF	neutrons ToF
Unit-cell dimensions (Å)	a = 4.6291(5) b = 5.4876(6) c = 18.5034(15)	a = 4.6254(8) b = 5.4798(10) c = 18.472(4)	a = 4.6284(3) b = 5.4903(4) c = 18.5131(13)	a = 4.6857(6) b = 5.5344(7) c = 18.673(2)	a = 4.64542(17) b = 5.48972(18) c =18.5494(8)	a = 4.64485(16) b = 5.49064(18) c =18.5445(8)
Volume (Å^3)	470.0(7)	468.2(7)	470.4(7)	484.2(7)	473.05(4)	472.95(3)
μ (mm^{-1})	1.878	1.869	1.872	2.112		
Crystal size (mm)	0.15 × 0.11 × 0.02	0.15 × 0.09 × 0.02	0.35 × 0.11 × 0.09	0.19 × 0.19 × 0.02	powder	powder
Theta range	4.40 to 30.02°	3.88 to 30.21°	3.87 to 30.02°	3.84 to 29.91°		
Index ranges (±h/±k/±l)	6/7/25					
Reflections collected	8621	8160	7568	8656		
Sys absence viol: n glide I >3σ	149	52	422	7		
Sys absence viol: c glide I >3σ	3	14	188	25		
Independent reflections	710 [R(int) = 0.0563]	721 [R(int) = 0.0668]	712 [R(int) = 0.0274]	730 [R(int) = 0.0735]		
Completeness to θ = 30.0°	99.70%	99.90%	99.90%	99.50%		
Absorption correction	Gaussian					
Max. / min. transmission	0.94812 / 0.78365	0.96947 / 0.77504	0.856 / 0.563	0.94751 / 0.71170		
Refinement method	Full-matrix least-squares on F^2				Rietveld	
Data / restraints / parameters	710 / 1 / 53	721 / 1 / 53	712 / 1 / 53	730 / 1 / 53	8216 (powder) /1/ 72	9650 /1/68
Goodness-of-fit on F^2, ψ^2	1.354	1.448	1.41	1.269	19.07	15.3
Final R indices	R1 = 0.0638	R1 = 0.0767	R1 = 0.0512	R1 = 0.0443		
[I >2σ(I)]	wR_2 = 0.1286	wR_2 = 0.1384	wR_2 = 0.1268	wR_2 = 0.0913		
R indices (all data)	R_1 = 0.0640 wR_2 = 0.1287	R_1 = 0.0848 wR_2 = 0.1408	R_1 = 0.0512 wR_2 = 0.1268	R_1 = 0.0528 wR_2 = 0.0942	R_1 = 0.0224 wR_2 = 0.0197	R_1 = 0.0128 wR_2 = 0.0132
Largest diff. peak and hole (e.Å^{-3})	0.95 and -0.75	1.00 and −1.00	1.17 and −1.88	0.69 and −0.72		

both the 90º ($\Delta d/d$ = 0.007) and 145º ($\Delta d/d$ = 0.005) detector banks. Refinements were performed using data from both detector banks simultaneously. The refined X-ray structure for *Pncm* was used as a starting model. Site occupancies were assigned to be the same as for the X-ray refinement, and all temperature factors were set to be isotropic. A March-Dollase preferred-orientation parameter was also included in the refinement to allow for the dominant platy {001} cleavage. Attempts to locate the missing H atom directly by difference-Fourier synthesis of the 293 K data were unsuccessful, so the approximate position of the H atom determined by single-crystal XRD was used and refined, along with U_{iso}. Refinement of the complete structure proceeded stably and gave an overall final wRp = 0.0197 for 8216 data. R_p was 0.0461 calculated for 4652 reflections in the 145º data and 0.0340 for 1901 reflections for the 90º data. The total weighted χ^2 was 19.1 for 72 variables, 46 experimental parameters and 26 structural parameters.

2 K dataset

Immediately after the 293 K experiment was completed, a second, longer experiment (46 h) was carried out at 1.7 K. Following this experiment, a dataset was collected for 30 min with the sample removed from the cryofurnace, and this dataset was used to apply a minor 'environmental background' correction to the sample dataset.

The H-free starting model used for refinement of the 90º and 145º 2 K datasets was that of the *Pncm* structure. The occupancy of the *T*2 site was fixed at 0.5 Si, 0.5 Al. In the full refinement of the complete structure (H included), 18 experimental parameters (scale factor, background, profile, March-Dollase preferred orientation, DIFA) were refined for each dataset, along with 25 structural parameters (coordinates, U_{iso}, fractional occupancy) and three unit-cell parameters, giving a total of 68 refined parameters. A cosine Fourier series was used to model the backgrounds. The 90º and 145º datasets contained 11391 and 9912 reflections, respectively. Initially, only the scale factor, background parameters, four profile parameters ($\sigma 1$, $\sigma 2$, $\gamma 1$, $\gamma 2$) and unit-cell parameters were refined to convergence, followed by atom coordinates. Details of partial (H-free) and complete refined structures are given in the Results section. As described below, it proved possible to locate the missing H atom from difference-Fourier synthesis of the combined 90º and 145º datasets. Furthermore, the location found independently by neutron powder diffraction is close to that determined by single-crystal XRD at 293 K.

Results and discussion

The microprobe analyses show that only two of the four samples contain Fe at the octahedral site (7%, tad1; 26% tad4). Sample tad5 shows trace amounts of Mn at 2(1) at.%. Sample tad2 is Fe- and Mn-free, within error.

Pncm structure: 293 K data

The unit-cell parameters for each sample (Table 1) are in general agreement with previously published studies (Papike and Zoltai, 1967; Peng *et al.*, 1959). Crystal tad4x1 (26% Fe at *M*1) has a larger unit cell, by ~2% in all directions, than the other samples, presumably due to the expansion of the octahedral site upon substitution of Fe for Al, which results in significant lengthening of *M*1–O bonds. In tad4x1, the *M*1–O1 bond length is 1.962(2) Å and the *M*1–OH bond length is 1.949(4) Å, whereas in the other samples, with $\leqslant$7% Fe, the octahedral bond lengths are all <1.93 Å (Table 3). Although Fe was found to be present only at the octahedral site (Artioli *et al.*, 1995; Akasaka *et al.*, 2003), the tetrahedral bond lengths also show a general lengthening with the greater Fe content in sample tad4x1. For example, the Si–O2 bond lengthens to 1.649(3) Å, whereas the other samples have an average Si–O2 bond length of 1.637 Å. Other bond lengths that follow the same trend include *T*2–O2, *T*2–O3, and Si–O1. The distortion parameters, angle-variance (AV) and quadratic-elongation (QE) of the framework polyhedra do not vary among the samples (Table 4). The unit-cell parameters and bond lengths in the remaining samples with <7% Fe show no significant variation with Mn or Fe content.

Greater Fe content in the prehnite structure appears to produce a fairly uniform expansion of the tetrahedral/octahedral framework. This is reflected in the geometry of the Ca site. Thus, within the area of the Ca channel, the distance between the Ca atoms is larger in tad4x1. The presence of a significant amount of Fe in the structure increases the Ca–Ca distance and lengthens Ca–O bond (Fig. 2, Table 3). The

TABLE 2. Positional and displacement parameters (Å^2) for prehnite in *Pncm.*

Sample ID Locality		tad1x2 Tyrol	tad2x1 Norway	tad5x1 South Africa	tad4x1 Mali	tad4 N Mali – 293 K	tad4 N Mali – 2 K
Ca1	z	0.0992(1)	0.0993(1)	0.0993(1)	0.0995(1)	0.10004(14)	0.09995(12)
	U_{iso}	0.013(1)	0.017(1)	0.010(1)	0.015(1)	0.0114(5)	0.0050(3)
	U_{11}	0.015(1)	0.018(1)	0.012(1)	0.017(1)		
	U_{22}	0.016(1)	0.016(1)	0.012(1)	0.014(1)		
	U_{33}	0.009(1)	0.016(1)	0.006(1)	0.013(1)		
	U_{12}	−0.002(1)	−0.001(1)	−0.001(1)	−0.001(1)		
	U_{13}	0	0	0	0		
	U_{23}	0	0	0	0		
*M*1	Al_{occup}	0.98(2)	1.00(2)	0.98(2)	0.77(1)	not refined	0.72(1)
	U_{iso}	0.010(1)	0.014(1)	0.008(1)	0.010(1)	0.0047(4)	0.0030(4)
	U_{11}	0.007(1)	0.010(2)	0.005(1)	0.007(1)		
	U_{22}	0.016(2)	0.016(2)	0.012(1)	0.012(1)		
	U_{33}	0.008(1)	0.016(2)	0.006(1)	0.012(1)		
	U_{12}	−0.001(1)	0.000(2)	−0.001(1)	−0.000(1)		
	U_{13}	0	0	0	0		
	U_{23}	0	0	0	0		
*T*2	x	0.1913(5)	0.1916(5)	0.1914(4)	0.1901(3)	0.1904(4)	0.1900(4)
	U_{iso}	0.009(1)	0.012(1)	0.005(1)	0.010(1)	0.0018(4)	0.00058(18)
	U_{11}	0.011(1)	0.012(1)	0.005(1)	0.008(1)		
	U_{22}	0.008(1)	0.008(1)	0.004(1)	0.009(1)		
	U_{33}	0.008(1)	0.016(1)	0.005(1)	0.012(1)		
	U_{12}	0	0	0	0		
	U_{13}	0	0	0	0		
	U_{23}	−0.000(1)	−0.000(1)	0.000(1)	0.001(1)		
Si1	z	0.1196(1)	0.1195(1)	0.1196(1)	0.1203(1)	0.12036(12)	0.12004(12)
	U_{iso}	0.009(1)	0.013(1)	0.006(1)	0.011(1)	0.0016(3)	0.00058(18)
	U_{11}	0.009(1)	0.011(1)	0.005(1)	0.008(1)		
	U_{22}	0.010(1)	0.012(1)	0.008(1)	0.011(1)		
	U_{33}	0.007(1)	0.015(1)	0.005(1)	0.013(1)		
	U_{12}	0.001(1)	0.001(1)	0.001(1)	0.000(1)		
	U_{13}	0	0	0	0		
	U_{23}	0	0	0	0		
O1	x	0.7504(8)	0.7512(8)	0.7502(7)	0.7487(5)	0.7489(3)	0.7484(3)
	y	0.1322(7)	0.1315(8)	0.1319(6)	0.1331(4)	0.13236(17)	0.13281(15)
	z	0.0735(2)	0.0734(2)	0.0734(2)	0.0742(1)	0.07436(8)	0.07395(7)
	U_{iso}	0.013(1)	0.015(1)	0.009(1)	0.014(1)	0.0065(2)	0.00314(15)
	U_{11}	0.012(2)	0.010(2)	0.006(1)	0.008(1)		
	U_{22}	0.018(2)	0.016(2)	0.013(2)	0.016(1)		
	U_{33}	0.010(2)	0.018(2)	0.009(1)	0.018(1)		
	U_{12}	−0.001(2)	−0.001(2)	−0.000(1)	−0.001(1)		
	U_{13}	0.002(2)	0.002(2)	0.002(1)	0.002(1)		
	U_{23}	0.000(1)	−0.000(2)	−0.001(1)	0.000(1)		
O2	x	0.3686(8)	0.3688(9)	0.3683(8)	0.3666(5)	0.3668(3)	0.3671(2)
	y	0.2143(7)	0.2142(7)	0.2143(6)	0.2138(5)	0.2147(3)	0.21464(19)
	z	0.1717(2)	0.1716(2)	0.1716(2)	0.1718(1)	0.17203(8)	0.17210(7)
	U_{iso}	0.015(1)	0.018(1)	0.012(1)	0.018(1)	0.0114(3)	0.00566(19)
	U_{11}	0.016(2)	0.017(2)	0.012(2)	0.017(1)		
	U_{22}	0.012(2)	0.012(2)	0.008(2)	0.013(1)		
	U_{33}	0.017(2)	0.026(2)	0.016(2)	0.025(1)		

TABLE 2 (*contd.*)

Sample ID Locality		tad1x2 Tyrol	tad2x1 Norway	tad5x1 South Africa	tad4x1 Mali	tad4 N Mali – 293 K	tad4 N Mali – 2 K
	U_{12}	−0.001(1)	−0.002(2)	−0.001(1)	−0.002(1)		
	U_{13}	0.008(1)	0.009(2)	0.009(1)	0.010(1)		
	U_{23}	−0.005(1)	−0.005(2)	−0.005(1)	−0.006(1)		
O3	z	0.2696(3)	0.2695(4)	0.2697(3)	0.26969(19)	0.26931(12)	0.26961(10)
	U_{iso}	0.016(1)	0.019(1)	0.014(1)	0.018(1)	0.0126(4)	0.0055(3)
	U_{11}	0.018(2)	0.022(3)	0.017(2)	0.020(2)		
	U_{22}	0.019(3)	0.017(3)	0.015(2)	0.019(2)		
	U_{33}	0.012(2)	0.019(3)	0.009(2)	0.015(2)		
	U_{12}	−0.004(2)	−0.004(3)	−0.004(2)	0.001(2)		
	U_{13}	0	0	0	0		
	U_{23}	0	0	0	0		
OH	x	0.2048(10)	0.2051(12)	0.2056(10)	0.2076(7)	0.2068(4)	0.2083(3)
	y	0.3021(9)	0.3020(11)	0.3021(9)	0.3053(6)	0.3077(4)	0.3071(3)
	U_{iso}	0.011(1)	0.014(1)	0.007(1)	0.014(1)	0.0087(4)	0.0046(3)
	U_{11}	0.006(2)	0.007(2)	0.004(2)	0.009(1)		
	U_{22}	0.015(2)	0.014(3)	0.010(2)	0.015(2)		
	U_{33}	0.011(2)	0.020(3)	0.008(2)	0.017(2)		
	U_{12}	−0.000(2)	−0.002(2)	−0.001(2)	−0.000(1)		
	U_{13}	0	0	0	0		
	U_{23}	0	0	0	0		
H	x	0.403(12)	0.41(1)	0.407(11)	0.402(8)	0.4125(7)	0.4142(6)
	y	0.25(3)	0.26(3)	0.25(3)	0.259(16)	0.2866(6)	0.2874(5)
	U_{iso}	0.06(4)	0.06(4)	0.06(4)	0.05(3)	0.0159(7)	0.0114(5)

General fractional coordinates for atoms: *M*1 (0 0 0), *T*2 (*x* 0.25 0.25), Si1 (0.5 0 *z*), Ca (0 0.5 *z*), O3 (0 0 *z*), OH and H (*x y* 0), O1 and O2 (*x y z*).
Symmetry operators: *x*, *y*, *z*; −*x*, −*y*, *z*; *x*, ½−*y*, ½+*z*; −*x*, ½+*y*, ½+*z*.

three O atoms surrounding the channel, OH, O1 and O3, are separated further from each other on opposite sides of the channel in tad4x1, with distances of 5.441(6) Å, 2.904(8) Å, and 8.601(8) Å respectively, as compared to values of ~5.39 Å, ~2.88 Å, and ~8.52 Å in the samples with smaller Fe contents. However, the ellipticity ratio of the Ca cavity remains constant.

The H atom in the structure was located approximately in the X-ray difference-Fourier maps on the O atom previously denoted 'OH', which is the otherwise underbonded oxygen as it is coordinated by only the *M*1 cation (Fig. 1). The H position lies on the (001) mirror plane and the O−H vector points away from the channel containing the calcium. This location for H was confirmed by the observation that the addition of the hydrogen atom into the structure reduced the weighted χ^2 of the refinement to the neutron powder diffraction data from 128 to 19.1. The coordinates of the H atom refined against the neutron diffraction data are 0.4125(7) 0.2866(6) 0, and the O(H)−H distance is 0.963(4) Å. The next closest O atoms are the two O1 atoms that are connected to a neighbouring octahedron, each with an O1···H distance of 2.25 Å. These two O1 atoms are the H-bond acceptors. As such, the O−H···O configuration is bifurcated. The total distance from OH−H···O1 is 3.03 Å, with an OH−H−O angle of 137.3º (Fig. 3).

Neutron powder diffraction: 2 K data

As mentioned above, the missing H atom could not be identified in difference-Fourier maps of the 293 K neutron data, but it was possible to refine its coordinates and U_{iso} by incorporating the approximate coordinates found by single-crystal XRD. However, data from the 2 K experiment allowed the direct location of the missing H atom

TABLE 3. Selected bond lengths and distances (Å) for prehnite in *Pncm*.

Sample ID Locality		tad1x2 Tyrol	tad2x1 Norway	tad5x1 South Africa	tad4x1 Mali	tad4 N Mali – 293 K	tad4 N Mali – 2 K
Bond lengths							
*M*1–O1	(×4)	1.926(4)	1.919(4)	1.925(3)	1.962(2)	1.9471(14)	1.9438(12)
*M*1–OH	(×2)	1.910(5)	1.907(6)	1.912(5)	1.949(4)	1.9434(17)	1.9439(15)
Poly. vol.		9.44	9.36	9.44	10.00	9.82	9.79
*T*2–O2	(×2)	1.677(4)	1.675(4)	1.678(4)	1.689(3)	1.6736(18)	1.6735(15)
*T*2–O3	(×2)	1.6727(19)	1.671(2)	1.6736(14)	1.6861(10)	1.6715(12)	1.6720(10)
Poly. vol.		2.34	2.34	2.35	2.40	2.33	2.33
Si1–O1	(×2)	1.612(4)	1.611(4)	1.612(4)	1.625(3)	1.6103(16)	1.6104(16)
Si1–O2	(×2)	1.638(4)	1.634(5)	1.638(4)	1.649(3)	1.6403(19)	1.6438(17)
Poly. vol.		2.19	2.18	2.19	2.24	2.19	2.19
Ca–O1	(×2)	2.374(4)	2.373(4)	2.377(4)	2.394(3)	2.3793(12)	2.3798(10)
Ca–O2	(×2)	2.677(4)	2.674(5)	2.675(4)	2.699(3)	2.6718(19)	2.6744(16)
Ca–O3		2.428(5)	2.425(6)	2.426(5)	2.443(4)	2.423(4)	2.419(3)
Ca–OH	(×2)	2.334(3)	2.332(4)	2.338(3)	2.357(2)	2.341(3)	2.3437(18)
OH–H		0.97(3)*	0.97(3)*	0.97(3)*	0.95(3)*	0.963(4)	0.963(3)
Distances							
Ca···Ca		3.671(3)	3.667(4)	3.677(3)	3.715(3)	3.711(5)	3.707(4)
O3···O3		8.526(11)	8.517(12)	8.53(1)	8.601(8)		
O1···O1		5.392(8)	5.391(9)	5.393(8)	5.441(6)		
OH...OH		2.883(11)	2.883(12)	2.89(1)	2.904(8)		
Ellipticity ratio							
O1···O1/O3···O3		0.632	0.633	0.632	0.633		
OH···OH/O3···O3		0.338	0.338	0.339	0.338		

* OH–H distance was constrained to 0.98±0.03 Å in X-ray refinement.

by difference-Fourier synthesis, as is now described.

In order to achieve convergence for the refinement of the H-free model it was necessary to refine an overall U_{iso} for the four non-equivalent oxygen atoms, an overall U_{iso} for the two T atoms and to fix the occupancy of the $^{[6]}$Al site at 1.0 Al. At convergence of this partial model, the agreement indices were (90/145/total): *R*p = 0.0357/0.0340/0.0348 and *wR*p = 0.0258/0.0247/0.0251. However, considerable unmodelled scattering intensity remained (Fig. 4*a*). After refinement of the H-free model structure (*Pncm*) to convergence, structure factors were extracted for difference-Fourier synthesis. A 3D difference-Fourier map of the prehnite unit cell was obtained by creating a .grd file in GSAS, This .grd file was then imported into the crystallographic structure visualization program *VESTA* (Momma and Izumi, 2008). Figure 5 is the difference-Fourier section at *x y* 0. The minima in the residual negative scattering density in the difference-Fourier map of prehnite are of a scale (−1 scattering unit) that is comparable to that used to locate missing H in difference-Fourier maps from neutron powder diffraction data for leucophoenicite (Welch *et al*., 2002) and akaganéite (Post *et al*., 2003 – Fig. 4). The deepest hole is −0.37 scattering units (s.u.) at 0.414 0.287 0 (Fig. 5) and is a plausible location for H, lying at 0.96 Å from the underbonded O(H) donor, which is also seen in the map as minor unmodelled residual negative scattering density. Adding this H atom to the 2 K refinement using these starting coordinates leads to stable refinement and major improvement (*Rp* decreases from 0.027 to 0.017, *wR*p from 0.037 to 0.019, weighted χ^2 reduces from 184 to 18). H

TABLE 4. Selected bond angles (°) and distortion parameters for prehnite in *Pncm*.

Sample ID Locality		tad1x2 Tyrol	tad2x1 Norway	tad5x1 South Africa	tad4x1 Mali	tad4 N Mali – 293 K	tad4 N Mali – 2 K
*M*1							
OH–*M*1–O1	(×4)	91.67(16)	91.59(18)	91.58(15)	91.49(11)	91.62(4)	91.50(4)
OH–*M*1–O1	(×4)	88.33(16)	88.41(18)	88.42(15)	88.51(11)	88.38(4)	88.50(4)
O1–*M*1–O1	(×2)	89.8(2)	89.9(2)	89.8(2)	89.89(15)	89.79(8)	89.74(7)
O1–*M*1–O1	(×2)	90.2(2)	90.1(2)	90.2(2)	90.11(15)	90.21(8)	90.26(7)
OH–*M*1–OH		180.0	180.0	180.0	180.0	180.0	180.0
O1–*M*1–O1	(×2)	180.0	180.0	180.0	180.0	180.0	180.0
AV		2.05	1.82	1.83	1.60	1.94	1.64
QE		1.0006	1.0005	1.0005	1.0005	1.0005	1.0005
*T*2							
O3–*T*2–O3		116.07(14)	115.94(17)	116.09(14)	116.22(11)	116.12(12)	116.27(10)
O3–*T*2–O2	(×2)	110.53(19)	110.4(2)	110.52(18)	110.48(14)	110.44(8)	110.61(7)
O3–*T*2–O2	(×2)	99.6(2)	99.8(2)	99.6(2)	99.64(15)	99.73(9)	99.61(7)
O2–*T*2–O2		121.4(3)	121.4(3)	121.6(3)	121.4(2)	121.37(16)	121.14(14)
AV		76.3	75.3	78.2	76.4	75.5	75.7
QE		1.0194	1.0192	1.0199	1.0195	1.0193	1.0193
Si1							
O1–Si1–O1		116.1(3)	116.1(3)	115.9(3)	116.14(19)	116.01(16)	115.88(15)
O1–Si1–O2	(×2)	111.56(19)	111.4(2)	111.55(18)	111.26(13)	111.28(6)	111.55(6)
O1–Si1–O2	(×2)	104.79(19)	104.9(2)	104.87(18)	104.80(13)	104.85(6)	104.84(5)
O2–Si1–O2		107.9(3)	107.9(3)	108.0(3)	108.5(2)	108.50(16)	108.07(15)
AV		19.8	19.0	18.9	19.0	18.7	19.2
QE		1.0047	1.0045	1.0045	1.0045	1.0045	1.0046
Ca							
OH–Ca–OH		76.3(2)	76.3(2)	76.32(19)	76.03(14)	75.12(11)	75.47(9)
O1–Ca–OH	(×2)	69.18(15)	69.07(18)	69.15(15)	70.13(11)	70.12(7)	70.10(6)
O1–Ca–OH	(×2)	92.33(16)	92.32(18)	92.21(15)	91.70(11)	91.29(8)	91.14(7)
O3–Ca–OH	(×2)	141.85(10)	141.83(12)	141.84(9)	141.99(7)	142.44(5)	142.26(5)
O2–Ca–OH	(×2)	157.72(13)	157.67(15)	157.71(12)	157.72(9)	157.23(10)	157.46(8)
O2–Ca–OH	(×2)	82.10(13)	82.01(15)	82.05(12)	82.17(9)	82.54(4)	82.40(4)
O1–Ca–O1		156.91(17)	156.8(2)	156.71(17)	157.30(13)	156.90(14)	156.62(12)
O3–Ca–O1	(×2)	101.55(9)	101.62(11)	101.64(8)	101.35(6)	101.55(7)	101.69(6)
O2–Ca–O1	(×2)	106.74(13)	106.85(15)	106.83(13)	106.44(10)	106.54(5)	106.53(4)
O2–Ca–O1	(×2)	84.98(13)	84.92(15)	84.97(13)	85.07(10)	85.15(4)	85.31(4)
O2–Ca–O3	(×2)	59.94(8)	60.01(10)	59.97(8)	59.95(6)	60.02(6)	59.98()5)
O2–Ca–O2		119.88(16)	120.01(19)	119.95(15)	119.90(12)	120.03(11)	119.95(9)
*T*2–O3–*T*2		155.0(3)	155.2(4)	154.9(3)	154.8(2)	155.25(15)	154.87(13)
*T*2–O2–Si1		140.7(2)	140.8(3)	140.7(2)	140.83(17)	140.61(10)	140.78(8)
*M*1–O1–Si1		129.5(2)	129.7(3)	129.5(2)	129.33(15)	129.58(6)	129.45(6)
Ca–O3–*T*2	(×2)	102.52(16)	102.42(19)	102.56(16)	102.60(12)	102.37(7)	102.56(6)
Ca–OH–*M*1	(×2)	101.68(16)	101.62(19)	101.57(15)	100.97(11)	100.90(5)	100.75(4)
Ca–OH–Ca		103.7(2)	103.7(2)	103.68(19)	103.97(14)	104.88(11)	104.53(9)
Ca–O2–Si1		111.26(19)	111.3(2)	111.33(18)	111.69(13)	111.71(11)	111.44(9)
Ca–O2–*T*2		93.02(17)	92.94(19)	93.07(16)	92.94(12)	92.97(9)	92.91(7)
Ca–O1–Si1		128.8(2)	128.6(2)	128.65(19)	129.30(14)	128.96(10)	128.90(9)
Ca–O1–*M*1		99.76(16)	99.86(17)	99.80(14)	99.34(10)	99.48(7)	99.52(6)
*M*1–OH–H						112.7(3)	113.4(2)

TABLE 5. Detailed results of single-crystal structure refinements for prehnite in *P*2*cm*.

Sample ID	tad1x2*	tad5x1*
Theta range	4.32 to 30.02º	3.87 to 30.02º
Index ranges $\pm h/\pm k/\pm l$	6/7/26	6/7/26
Reflections collected	9160	8069
Independent reflections	1407 [R(int) = 0.0553]	1410 [R(int) = 0.0268]
Completeness to θ = 30.00º	99.60%	99.70%
Absorption correction	Gaussian	
Max. /min. transmission	0.94812 and 0.78365	0.856 and 0.563
Refinement method	Full-matrix least-squares on F^2	
Data / restraints / parameters	1407 / 3 / 82	1410 / 3 / 82
Goodness-of-fit on F^2	1.221	1.286
Final R indices [$I > 2\sigma(I)$]	R_1 = 0.0435, wR_2 = 0.0972	R_1 = 0.0197, wR_2 = 0.0559
R indices (all data)	R_1 = 0.0454, wR_2 = 0.0972	R_1 = 0.0198, wR_2 = 0.0560
Absolute structure parameter	0.17(11)	0.18(6)
Largest diff. peak and hole	0.770 and −0.650 e.Å^{-3}	0.330 and −0.420 e.Å^{-3}

* See Table 1 for crystal-specific values (crystal size, microprobe results, unit-cell parameters, density, absorption, etc.).

coordinates refine to x = 0.4143(6) and y = 0.2878(5), with U_{iso} = 0.0114(5) Å^2. The O–H bond is 0.963(3) Å long and the H···O1 distance is 2.241 Å.

For the rest of the structure, the U_{iso} of all atoms, with the exceptions of the two *T* sites, were refined independently. When the U_{iso} of two *T* sites were refined separately they became marginally non-positive definite. As this result is unphysical, an overall U_{iso} for the pair of *T* sites was refined and gave a satisfactory result (0.0006 Å^2). There is excellent agreement between the analytical (0.74 Al + 0.26 Fe) and refined (0.72 Al + 0.28 Fe) site occupancies of the $^{[6]}$Al site. Final agreement indices for refinement of the complete structure are (90/145/total): *R*p = 0.0128/0.0174/0.0153 and *wR*p = 0.0113/0.0142/0.0132, with a final weighted χ^2 of 15.3. Final $R(F^2)$ values for the 90º and 145º datasets are 0.040 (11391 reflections) and 0.050 (9912 reflections), respectively. The final Rietveld refinement for the 2 K 90º dataset is shown in Fig. 4*b*. Coordinates of Ca, Al, O and *T*-site atoms for the 2 K structure are very close to those determined by single-crystal XRD at 293 K. Furthermore, the H position is also in good agreement with its location in the 293 K structure. Overall, the X-ray and neutron data have provided

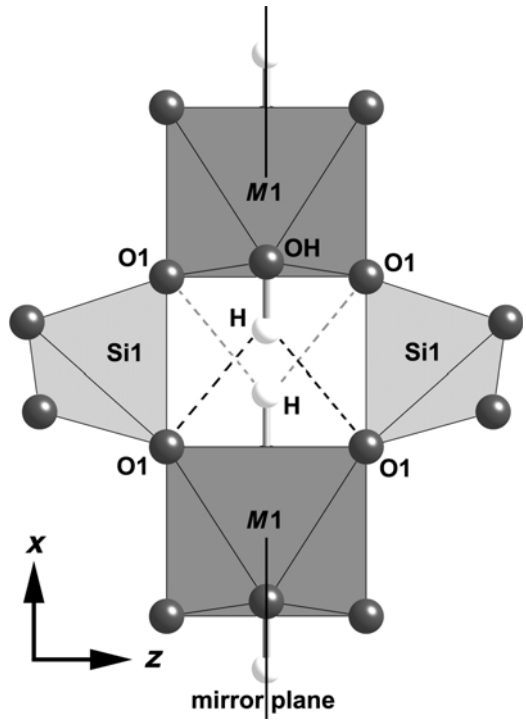

FIG. 3. The H environment in prehnite as viewed from [010]. The small grey spheres represent O sites and the small white spheres represent H sites. The heavy dash shows the bifurcated environment of the H and the next nearest oxygen, O1. The light dash shows the bifurcated environment of the H and O1 on the lower apex of the octahedron.

a coherent, complete structure model for the average structure of prehnite.

P2cm

In space group *Pncm*, which corresponds to the average Al-Si disordered structure, the tetrahedral site occupancies are $T1$ = Si and $T2$ = $Al_{0.5}Si_{0.5}$. Papike and Zoltai (1967) showed that there are only three ordering patterns for Al/Si on the $T2$ site with space group symmetries *P2cm* (acentric), *P2/n* (centric), and $P22_12$ (acentric). Space group $P22_12$ leads to Al−O−Al linkages and so is considered unlikely to occur (cf. Lowenstein, 1954), and no crystal-chemical evidence for this space group has ever been found. The other two space groups, *P2cm* and *P2/n*, can be distinguished by the presence of systematic absence violations of the *n* and *c* glides of *Pncm*, respectively. It was found that the single-crystal XRD pattern from crystal tad1x2 had 149 violations of the *n*-glide condition and just 3 of

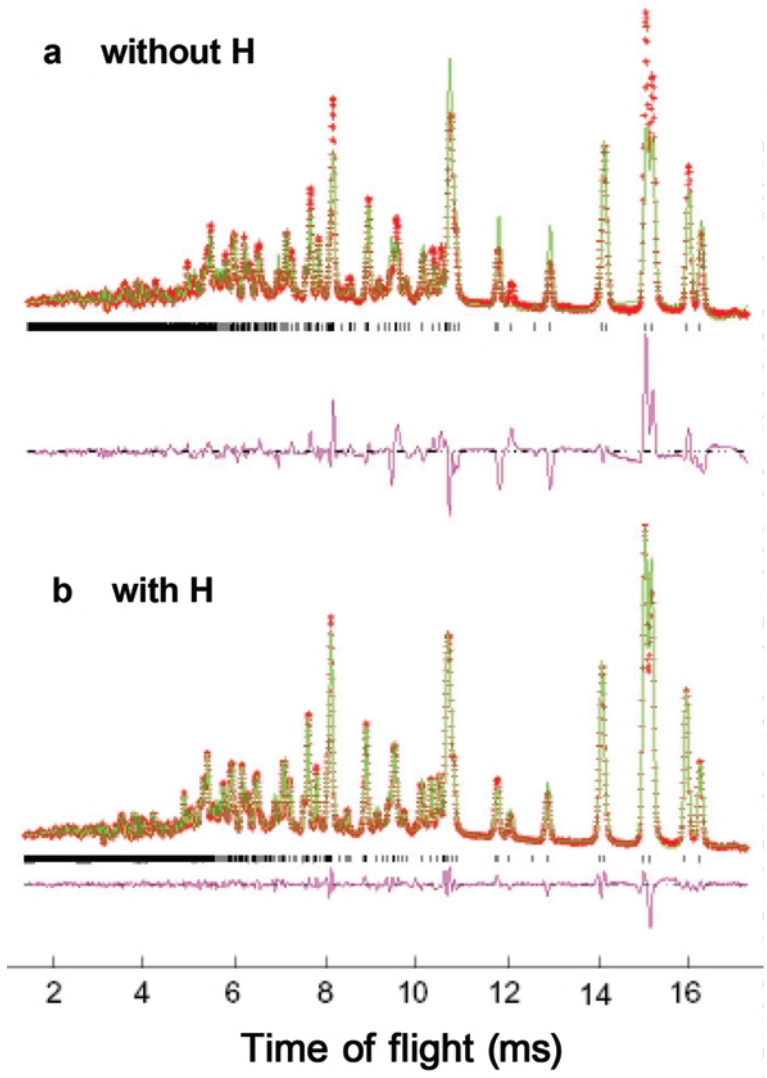

FIG. 4. Results of Rietveld refinements of the 2K Polaris data for prehnite (*Pncm*) for the 90º detector bank (*a*) without H, and (*b*) with H included in the structure model. The significant improvement of the fit, obtained by including H, is especially obvious in the region 11−17 ms.

TABLE 6. Positional and displacement parameters (Å^2) for prehnite in *P*2*cm*.

Sample ID Locality		tad1x2 Tyrol	tad5x1 South Africa			tad1x2 Tyrol	tad5x1 South Africa
Ca1	x	0.0033(5)	0.0051(3)		U_{11}	0.014(1)	0.007(1)
	y	0.48876(15)	0.48913(8)		U_{22}	0.015(1)	0.011(1)
	z	0.09922(3)	0.09931(2)		U_{33}	0.011(1)	0.009(1)
	U_{iso}	0.013(1)	0.009(1)		U_{12}	−0.001(1)	−0.001(1)
	U_{11}	0.017(1)	0.012(1)		U_{13}	0.002(1)	0.002(1)
	U_{22}	0.013(1)	0.009(1)		U_{23}	−0.001(1)	−0.000(1)
	U_{33}	0.009(1)	0.007(1)				
	U_{12}	−0.001(1)	−0.000(1)	O1b	x	0.2551(9)	0.2538(4)
	U_{13}	−0.001(1)	−0.001(1)		y	0.8550(6)	0.8560(3)
	U_{23}	−0.000(1)	0.000(1)		z	0.92648(15)	0.92670(9)
					U_{iso}	0.013(1)	0.009(1)
*M*1	x	0.0016(8)	0.0026(4)		U_{11}	0.014(1)	0.007(1)
	y	−0.0128(4)	−0.01228(17)		U_{22}	0.015(1)	0.011(1)
	U_{iso}	0.009(1)	0.006(1)		U_{33}	0.011(1)	0.009(1)
	U_{11}	0.008(1)	0.005(1)		U_{12}	−0.001(1)	−0.001(1)
	U_{22}	0.012(1)	0.008(1)		U_{13}	0.002(1)	0.002(1)
	U_{33}	0.008(1)	0.006(1)		U_{23}	−0.001(1)	−0.000(1)
	U_{12}	−0.001(1)	0.000(1)				
	U_{13}	0	0	O2a	x	0.3585(9)	0.3573(5)
	U_{23}	0	0		y	0.2210(6)	0.2200(3)
					z	0.16697(15)	0.16728(9)
Si1	x	0.4952(6)	0.4964(3)		U_{iso}	0.014(1)	0.011(1)
	y	−0.0009(3)	−0.00101(11)		U_{11}	0.016(1)	0.011(1)
	z	0.11954(4)	0.11953(2)		U_{22}	0.016(1)	0.011(1)
	U_{iso}	0.009(1)	0.006(1)		U_{33}	0.010(1)	0.010(1)
	U_{11}	0.009(1)	0.005(1)		U_{12}	0.001(1)	−0.000(1)
	U_{22}	0.011(1)	0.008(1)		U_{13}	0.004(1)	0.004(1)
	U_{33}	0.008(1)	0.005(1)		U_{23}	−0.001(1)	−0.003(1)
	U_{12}	0.000(1)	0.000(1)				
	U_{13}	0.002(1)	0.001(1)	O2b	x	0.6211(9)	0.6207(5)
	U_{23}	0.000(1)	−0.000(1)		y	0.7900(6)	0.7893(3)
					z	0.82365(16)	0.82418(9)
*T*2A	x	0.1892(5)	0.1888(3)		U_{iso}	0.014(1)	0.011(1)
	U_{iso}	0.011(1)	0.006(1)		U_{11}	0.016(1)	0.011(1)
	U_{11}	0.012(1)	0.006(1)		U_{22}	0.016(1)	0.011(1)
	U_{22}	0.011(1)	0.007(1)		U_{33}	0.010(1)	0.010(1)
	U_{33}	0.009(1)	0.006(1)		U_{12}	0.001(1)	−0.000(1)
	U_{12}	0	0		U_{13}	0.004(1)	0.004(1)
	U_{13}	0	0		U_{23}	−0.001(1)	−0.003(1)
	U_{23}	−0.002(1)	−0.000(1)				
				O3	x	−0.0113(13)	−0.0096(7)
*T*2S	x	−0.1935(4)	−0.1940(3)		y	−0.0099(6)	−0.0102(3)
	U_{iso}	0.011(1)	0.006(1)		z	0.26948(13)	0.26970(8)
	U_{11}	0.012(1)	0.006(1)		U_{iso}	0.015(1)	0.012(1)
	U_{22}	0.012(1)	0.007(1)		U_{11}	0.016(1)	0.013(1)
	U_{33}	0.009(1)	0.006(1)		U_{22}	0.016(1)	0.012(1)
	U_{12}	0	0		U_{33}	0.013(1)	0.010(1)
	U_{13}	0	0		U_{12}	−0.005(2)	−0.004(1)
	U_{23}	0.001(1)	−0.000(1)		U_{13}	0.001(3)	0.000(1)
					U_{23}	−0.001(2)	−0.001(1)
O1a	x	0.7552(9)	0.7544(5)				
	y	0.1196(6)	0.1201(3)	OHa	x	0.2094(11)	0.2095(6)
	z	0.07347(16)	0.07340(9)		y	0.2877(9)	0.2900(5)
	U_{iso}	0.013(1)	0.009(1)		U_{iso}	0.012(1)	0.008(1)

TABLE 6 (*contd.*).

Sample ID Locality		tad1x2 Tyrol	tad5x1 South Africa
	U_{11}	0.008(1)	0.005(1)
	U_{22}	0.015(1)	0.010(1)
	U_{33}	0.011(1)	0.010(1)
	U_{12}	0.001(1)	−0.000(1)
	U_{13}	0	0
	U_{23}	0	0
OHb	*x*	0.7990(12)	0.7973(6)
	y	0.6848(9)	0.6863(5)
	U_{iso}	0.012(1)	0.008(1)
	U_{11}	0.008(1)	0.005(1)
	U_{22}	0.015(1)	0.010(1)
	U_{33}	0.011(1)	0.010(1)
	U_{12}	0.001(1)	−0.000(1)
	U_{13}	0	0
	U_{23}	0	0
Ha	*x*	0.413(7)	0.400(7)
	y	0.287(17)	0.254(11)
	U_{iso}	0.04(2)	0.035(9)
Hb	*x*	0.600(8)	0.605(7)
	y	0.722(16)	0.711(11)
	U_{iso}	0.04(2)	0.035(9)

General fractional coordinates for atoms: *M*1 (*x y* 0), *T*2A (*x* 0.25 0.25), *T*2S (*x* 0.75 0.75), OHa, OHb, Ha and Hb (*x y* 0), Ca, O1a, O1b, O2a, O2b, O3, and Si1 (*x y z*). Displacement parameters for split sites (i.e. *T*2A and *T*2S, O1a and O1b, O2a and O2b, OHa and OHb, Ha and Hb) were constrained to be equal.
Origin of space group shifted to correspond to that of *Pncm*. Symmetry operators: *x*, *y*, *z*; *x*, *y*, −*z*; *x*, ½−*y*, ½−*z*; *x*, ½−*y*, ½+*z*.

TABLE 7. Selected bond lengths and distances (Å) for prehnite in *P*2*cm*.

Sample ID Locality		tad1x2 Tyrol	tad5x1 South Africa
Bond lengths			
*M*1−O1a	(×2)	1.917(4)	1.922(2)
*M*1−O1b	(×2)	1.938(4)	1.928(2)
*M*1−OHa		1.909(6)	1.916(3)
*M*1−OHb		1.906(6)	1.908(3)
Poly. vol.		9.441	9.440
*T*2A−O2a	(×2)	1.732(4)	1.7263(18)
*T*2A−O3	(×2)	1.739(5)	1.737(3)
Poly. vol.		2.566	2.545
*T*2S−O2b	(×2)	1.625(3)	1.6333(19)
*T*2S−O3	(×2)	1.606(5)	1.611(3)
Poly. vol.		2.127	2.152
Si1−O1a		1.616(5)	1.612(3)
Si1−O1b		1.608(4)	1.616(2)
Si1−O2a		1.628(4)	1.6334(19)
Si1−O2b		1.662(3)	1.6562(18)
Poly. vol.		2.201	2.204
Ca−O1a		2.377(4)	2.3833(18)
Ca−O1b		2.372(4)	2.3695(18)
Ca−O2a		2.537(4)	2.535(2)
Ca−O2b		2.811(4)	2.808(2)
Ca−O3		2.433(3)	2.4287(15)
Ca−OHa		2.345(4)	2.3391(17)
Ca−OHb		2.328(4)	2.3404(18)
OHa−Ha		0.94(3)*	0.90(3)*
OHb−Hb		0.94(3)*	0.90(3)*
Distances			
Ca···Ca		3.672(13)	3.6772(7)
O3···O3		8.531(5)	8.527(3)
O1a···O1b		5.389(4)	5.3916(18)
OHa...OHb		2.891(5)	2.894(3)
Ellipticity ratio			
O1a···O1b/O3···O3		0.632	0.632
OHa···OHb/O3···O3		0.339	0.339

* OH−H distance was constrained to 0.98±0.03 Å in refinement.

the *c*-glide voliations. Crystal tad5x1 had 422 violations of the *n*-glide condition and 188 of the *c*-glide violations. The violations therefore suggest that the dominant ordering pattern has *P*2*cm* symmetry. The remaining crystals, tad2x1 and tad4x1, each show <60 systematic absence violations so the limited data did not allow refinement of an ordered structure model. Therefore, refinements of tad1x2 and tad5x1 were performed in *P*2*cm*, and the results from tad5x1 are discussed here. Results from tad1x2 are the same within the (larger) esds.

For a change in symmetry from *Pncm* to *P*2*cm*, the atom sites *T*2, O1, O2, OH and H split to become two unique sites each. The octahedral *M*1 site, at Wyckoff position 2*a* in *Pncm* lies at Wyckoff position 2*c* in *P*2*cm*. The disordered *T*2 site (4*g* in *Pncm*) splits into an Al-rich site (*T*2A), sitting Wyckoff position 2*b* in *P*2*cm*, and a Si-rich site (*T*2S) at Wyckoff position 2*a*. OH and H positions at Wyckoff position 4*h* in *Pncm* each split into two non-equivalent sites (OHa, OHb,

TABLE 8. Selected bond angles (º) and distortion parameters for prehnite in *P*2*cm*.

Sample ID		tad1x2	tad5x1			tad1x2	tad5x1
Locality		Tyrol	South Africa			Tyrol	South Africa
*M*1							
OHb−*M*1−O1a	(×2)	92.1(2)	91.74(10)	O1b−Ca−O1a		156.86(8)	156.66(5)
OHa−*M*1−O1a	(×2)	88.42(16)	88.35(8)	OHb−Ca−O3		138.93(15)	138.67(8)
OHb−*M*1−O1b	(×2)	88.41(16)	88.57(8)	OHa−Ca−O3		144.65(15)	144.92(8)
OHa−*M*1−O1b	(×2)	91.04(19)	91.34(10)	O1b−Ca−O3		100.00(12)	100.14(6)
O1a−*M*1−O1a		90.3(3)	89.98(12)	O1a−Ca−O3		103.14(12)	103.17(7)
O1a−*M*1−O1b	(×2)	90.25(9)	90.26(5)	OHb−Ca−O2a		157.01(15)	157.51(8)
O1b−*M*1−O1b		89.2(3)	89.49(12)	OHa−Ca−O2a		81.41(13)	81.81(7)
O1a−*M*1−O1b	(×2)	179.2(3)	179.60(13)	O1b−Ca−O2a		105.77(15)	106.50(8)
OHb−*M*1−OHa		179.2(4)	179.88(18)	O1a−Ca−O2a		85.32(11)	85.26(6)
AV		1.99	1.78	O3−Ca−O2a		63.40(12)	63.26(7)
QE		1.0006	1.0005	OHb−Ca−O2b		82.70(13)	82.21(7)
				OHa−Ca−O2b		158.49(14)	157.97(8)
*T*2A				O1b−Ca−O2b		84.99(11)	84.92(6)
O2a−*T*2A−O2a		126.2(3)	126.30(15)	O1a−Ca−O2b		107.39(15)	106.98(8)
O2a−*T*2A−O3	(×2)	97.65(15)	97.54(8)	O3−Ca−O2b		56.46(12)	56.69(6)
O2a−*T*2A−O3	(×2)	110.47(14)	110.27(8)	O2a−Ca−O2b		119.86(7)	119.94(4)
O3−*T*2A−O3		115.5(5)	116.2(3)				
AV		119.5	122.7	O−central angles			
QE		1.0303	1.0313	Si1−O1a−*M*1		131.45(19)	131.40(10)
				Si1−O1a−Ca		127.05(17)	127.21(9)
*T*2S				*M*1−O1a−Ca		100.23(18)	99.96(9)
O3−*T*2S−O3		116.6(5)	116.0(3)	Si1−O1b−*M*1		127.33(18)	127.58(10)
O3−*T*2S−O2b	(×2)	110.78(16)	111.13(9)	Si1−O1b−Ca		130.56(17)	130.02(9)
O3−*T*2S−O2b	(×2)	101.53(16)	101.28(9)	*M*1−O1b−Ca		99.23(18)	99.73(9)
O2b−*T*2S−O2b		116.3(3)	116.67(15)				
AV		45.3	46.7	Si1−O2a−*T*2A		136.28(19)	136.82(11)
QE		1.0115	1.0118	Si1−O2a−Ca		114.74(16)	114.70(9)
				*T*2A−O2a−Ca		95.27(16)	95.40(9)
Si1				*T*2S−O2b−Si1		144.0(3)	143.44(12)
O1a−Si1−O1b		115.88(12)	115.78(7)	*T*2S−O2b−Ca		90.79(15)	90.81(8)
O1a−Si1−O2a		105.55(18)	105.81(10)	Si1−O2b−Ca		107.81(15)	108.10(9)
O1b−Si1−O2a		112.6(3)	111.94(13)				
O1a−Si1−O2b		110.8(3)	111.27(14)	*T*2S−O3−*T*2A		155.06(17)	154.79(9)
O1b−Si1−O2b		103.75(18)	103.72(10)	*T*2S−O3−Ca		106.14(15)	106.24(8)
O2a−Si1−O2b		108.15(13)	108.23(7)	*T*2A−O3−Ca		98.80(14)	98.96(8)
AV		20.5	19.4				
QE		1.0049	1.0047	*M*1−OHa−Ca	(×2)	101.63(19)	101.69(10)
				Ca−OHa−Ca		103.1(2)	103.63(11)
Ca				*M*1−OHa−Ha		120(6)	107(4)
OHb−Ca−OHa		76.43(9)	76.41(5)				
OHb−Ca−O1b		69.52(15)	69.31(8)	*M*1−OHb−Ca	(×2)	101.67(19)	101.34(10)
OHa−Ca−O1b		92.40(15)	92.35(8)	Ca−OHb−Ca		104.1(2)	103.55(11)
OHb−Ca−O1a		92.25(16)	92.01(8)	*M*1−OHb−Hb		107(6)	111(4)
OHa−Ca−O1a		68.81(15)	68.98(8)				

Ha, and Hb), all having Wyckoff position 2*c* in *P*2*cm*. The Ca atom, previously located on Wyckoff position 4*e*, is a GEP (i.e. general equivalent position) in *P*2*cm*, as are O1a, O1b, O2a, O2b and O3. In the *P*2*cm* refinements, it was found necessary to constrain the oxygen anisotropic displacement parameters (U_{ij}) of the pairs of split oxygen sites to be equal in order for the refinement to remain stable.

The most significant structural change upon reducing the symmetry from *Pncm* to *P*2*cm* is the distinction between the *T*2A and *T*2S sites, as is clearly apparent in both refinements, with a *T*2S−O average bond length of 1.622 Å and a

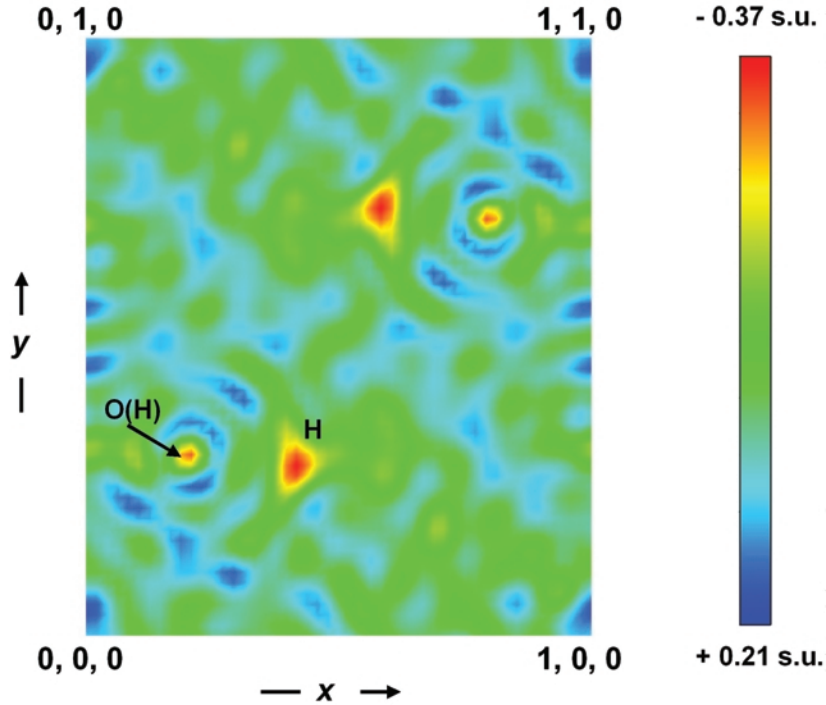

FIG. 5. Difference-Fourier section at $x\ y\ 0$ for prehnite. The octahedrally-coordinated Al atom is located at 0, 0, 0, at which there is residual unmodelled scattering density. The position of the missing H atom is indicated at 0.414, 0.287, 0. Unmodelled residual scattering density associated with the OH oxygen is also indicated. The residual scattering density ranges from −0.37 to +0.21 s.u.

*T*2A−O average bond length of 1.732 Å (Table 7), which are in agreement with those previously published (Balić-Žunić *et al.*, 1990). The bond lengths suggest full Al,Si ordering on the *T*2 site.

In *P*2*cm*, the *T*1 site does not split and remains fully occupied by Si; however, the site symmetry is reduced from 2 to 1. Nonetheless, there are significant changes in the geometry of this tetrahedron as a consequence of the ordering of Al and Si on *T*2 (*T*2A, *T*2S). The Si−O2b bond becomes longer at 1.6562(18) Å, because the O2b atom is bonded to the *T*2S site, containing Si. Conversely, the Si−O2a bond is shorter because the O2a atom is bonded to the Al-containing *T*2A site. The same patterns of tetrahedral distortions due to neighbouring tetrahedral sites occur in feldspars (Phillips and Ribbe, 1973; Angel *et al.*, 1990) and reflect the need for local charge balance at the bridging oxygen atom. For the same reason the Si−O2a−*T*2A is reduced from an average of 140.7(2)° in *Pncm* to 136.82(11)° and the Si−O2b−*T*2S angle is increased to 143.44(12)° (*cf.* Geisinger *et al.*, 1985). The Si−O1a and Si−O1b bonds remain unchanged, because the O1 oxygen atoms form the bridge to the octahedral site (Table 7).

The Ca atom, sitting on a site with two-fold symmetry in *Pncm*, becomes a GEP in *P*2*cm*, and so each Ca−O bond is unique. The largest changes occur in the length of Ca−O2 bonds and angles which again can be interpreted as a consequence of ordering of Al and Si on the *T*2 site and the need to maintain local charge balance of oxygens. The Ca−O2b bond length increases from 2.675(4) Å in *Pncm* to 2.808(2) Å in *P*2*cm*, because the O2b atom is bonded to the Si-containing *T*2S site, while the Ca−O2a bond decreases to 2.535(2) Å, due to the O2a atom being bonded to *T*2A (Fig. 2, Table 7). There are associated minor changes in bond angles, especially those involving O2.

The *M*1 octahedral site, containing Al and Fe, lying on a centre of symmetry and having 2/*m* point symmetry in *Pncm*, lies on a mirror in *P*2*cm* (acentric). Consequently, the *M*1 site is coordi-

nated to two O1a, two O1b, OHa and OHb. However, because the symmetry-breaking process (Al, Si ordering on *T*2) is not directly associated with changes on the octahedral site, there are only small changes in its geometry. The bond length *M*1−O1a decreases to 1.917(4) Å and *M*1−O1b increases to 1.938(4) Å in sample tad1x2 while in sample tad5x1 both bond lengths remain the same as *Pncm* values (1.925(3) Å). This small difference may reflect the different octahedral site occupancies (Table 1). The *M*1−OHa and *M*1−OHb bond lengths change from an average *Pncm* value of 1.912(5) Å to 1.916(3) Å and 1.908(3) Å in *P*2*cm*.

For the 293 K structure, H atoms were located approximately in difference-Fourier maps using only X-ray data (no neutron data were collected for sample tad5). In the *P*2*cm* structure, loss of the centre of symmetry results in two non-equivalent H atoms (Ha and Hb) on opposite apices of the *M*1 octahedron. Atoms Ha and Hb retain *m* point symmetry and each has a different pair of symmetry-equivalent O1 atoms (O1a or O1b) of the adjacent octahedron as hydrogen-bond acceptors. Therefore, the bifurcated hydrogen bonding in prehnite is not an artifact of averaging in space group *Pncm* but is present in the true local *P*2*cm* symmetry of the structure.

Conclusions

Neutron powder diffraction at 2 K and 293 K and single-crystal XRD data at 293 K have allowed the first complete structure model to be obtained for prehnite. The H atom position of the *Pncm* structure was located using difference-Fourier maps constructed from neutron powder diffraction data collected at 2 K and single-crystal XRD data at 293 K. It has been established that the H atom is located on the Al octahedron, attached to the OH atom in agreement with bond-valence calculations. The O−H vector points away from the adjacent Ca atoms. Symmetry requires that, if the H participates in a hydrogen bond, then it must be bifurcated and involve two O atoms on one adjacent octahedron.

All four prehnite crystals studied here by XRD have an average structure with *Pncm* symmetry, but all show evidence, to a greater or lesser degree, of Al,Si ordering in the form of violations of both the *c* and *n* glides. Given that the number of *n*-glide violations often exceeds those of the *c* glide, it appears that the ordering pattern with *P*2*cm* symmetry is the dominant one in all of the prehnite samples examined here. The fact that the two samples which could be refined in the ordered *P*2*cm* symmetry appear to have fully-ordered distributions of Al and Si, suggests that all natural prehnites may have completely ordered Al/Si distributions, at least on a local length-scale.

Acknowledgements

We thank Dr R. Pagano (Milano, Italy) for providing sample tad5 used in this study, and the Natural History Museum (London) for providing samples tad1 and tad2. The microprobe analyses for samples tad1, tad2 and tad4 were performed by Clayton Loehn at the Virginia Tech Microprobe Laboratory, while that for sample tad5 was performed by Dr G.D. Gatta (Milano, Italy). Thanks are due to Ron Smith for assistance with neutron powder diffraction on the POLARIS instrument at ISIS. The award of ISIS beamtime is gratefully acknowledged. The X-ray diffraction studies were performed at Virginia Tech, with the support of NSF grants EAR-0408460 and EAR-0738692 to N.L. Ross and R.J. Angel. Thanks are also due to reviewers J. Loveday, F. Cámara and L. Bindi.

References

Akasaka, M., Hashimoto, H., Makino, K. and Hino, R. (2003) ^{57}Fe Mossbauer and X-ray Rietveld studies of ferrian prehnite from Kouragahana, Shimane Peninsula, Japan. *Journal of Mineralogical and Petrological Sciences*, **98**, 31−40.

Akizuki, M. (1987) Al,Si order and the internal texture of prehnite. *The Canadian Mineralogist*, **25**, 707−716.

Angel, R.J., Carpenter, M.A. and Finger, L.W. (1990) Structural variation associated with the compositional variation and order-disorder behavior in anorthite-rich feldspars. *American Mineralogist*, **75**, 150−162.

Artioli, G., Quartieri, S. and Deriu, A. (1995) Spectroscopic data on coexisting prehnite-pumpellyite and epidote-pumpellyite. *The Canadian Mineralogist*, **33**, 67−75.

Aumento, F. (1968) The space group of prehnite. *The Canadian Mineralogist*, **9**, 485−492.

Balić-Žunić, T., Šćavničar, S. and Molin, G. (1990) Crystal structure of prehnite from Komiža. *European Journal of Mineralogy*, **2**, 731−734.

Baur, W.H., and Hofmeister, W. (1990) Prehnite: structural similarity of the monoclinic and orthorhombic polymorphs and their Si/Al ordering. *Journal of Solid State Chemistry*, **86**, 330−333.

Berry, A.J. and James, M. (2002) Refinement of hydrogen positions in natural chondrodite by powder neutron diffraction: implications for the stability of humite minerals. *Mineralogical Magazine*, **66**, 441–449.

Farrugia, L.J. (1999) WinGX suite for small-molecule single-crystal crystallography. *Journal of Applied Crystallography*, **32**, 837–838.

Geisinger, K.L., Gibbs, G.V. and Navrotsky, A. (1985) A molecular orbital study of bond length and angle variations in framework silicates. *Physics and Chemistry of Minerals*, **11**, 266–283.

Larson, A.C. and Von Dreele, R.B. (2000) GSAS-General Structure Analysis System. *Los Alamos National Laboratory*, LAUR-86-748.

Lowenstein, W. (1954) The distribution of aluminum in the tetrahedra of silicates and aluminates. *American Mineralogist*, **39**, 92–96.

Momma K. and Izumi, F. (2008) VESTA: a three-dimensional visualization system for electronic and structural analysis. *Journal of Applied Crystallography*, **41**, 653–658.

Nuffield, E.W. (1943) Prehnite from Ashcroft, British Columbia. *University of Toronto Studies*, **48**, 49–64.

Papike, J.J. and Zoltai, T. (1967) Ordering of tetrahedral aluminum in prehnite $Ca_2(AlFe^{+3})[Si_3AlO_{10}](OH)_2$. *American Mineralogist*, **52**, 974–984.

Peng, S.-T., Chou, K.-D. and Tang, Y.-C. (1959) The structure of prehnite. *Acta Chemistry Sinica*, **25**, 56–63.

Phillips, M.W. and Ribbe, P.H. (1973) The variation of tetrahedral bond lengths in sodic plagioclase feldspars. *Contributions to Mineralogy and Petrology*, **39**, 327–339.

Post, J.E., Heaney, P.J., Von Dreele, R.B. and Hanson, J.C. (2003) Neutron and temperature-resolved synchrotron powder diffraction study of akaganeite. *American Mineralogist*, **88**, 782–788.

Preisinger, A. (1965) Prehnit – ein neuer Schichtsilikattyp. *Tschermaks Mineralogische und Petrographische Mitteilungen*, **10**, 491–504.

Salvadó, M.A., Pertierra, P., García-Granda, S., García, J.R., Rodríguez, J. and Fernández-Díaz, M.T. (1996) Neutron powder diffraction study of α-$Ti(HPO_4)_2.H_2O$ and α-$Hf(HPO_4)_2.H_2O$; H-atom positions. *Acta Crystallographica B*, **52**, 896–898.

Sheldrick, G.M. (2008) A short history of SHELX. *Acta Crystallographica A*, **64**, 112–122.

Traube, H. (1894) Über die pyroelecktrischen Eigenschaften und die Krystallform des Prehnits. *Neues Jahrbuch für Mineralogie*, **9**, 134–146.

Welch, M.D., Marshall, W.G., Ross, N.L. and Knight, K.S. (2002) H positions in leucophoenicite, $Mn_7Si_3O_{12}(OH)_2$: A close relative of the hydrous B phases. *American Mineralogist*, **87**, 154–159.